# Signaling Pathways Crucial for Craniofacial Development Revealed by Endothelin-A Receptor-Deficient Mice

**David E. Clouthier,**\*,† **S. Clay Williams,**\*,† **Hiromi Yanagisawa,**\*,†
**Matthew Wieduwilt,**\*,† **James A. Richardson,**‡
**and Masashi Yanagisawa**\*,†,[1]

\*Howard Hughes Medical Institute, †Department of Molecular Genetics, and ‡Department of
Pathology, University of Texas Southwestern Medical Center at Dallas,
5323 Harry Hines Boulevard, Dallas, Texas 75235

Most of the bone and cartilage in the craniofacial region is derived from cephalic neural crest cells, which undergo three primary developmental events: migration from the rhombomeric neuroectoderm to the pharyngeal arches, proliferation as the ectomesenchyme within the arches, and differentiation into terminal structures. Interactions between the ectomesenchymal cells and surrounding cells are required in these processes, in which defects can lead to craniofacial malformation. We have previously shown that the G-protein-coupled endothelin-A receptor ($ET_A$) is expressed in the neural crest-derived ectomesenchyme, whereas the cognate ligand for $ET_A$, endothelin-1 (ET-1), is expressed in arch epithelium and the paraxial mesoderm-derived arch core; absence of either $ET_A$ or ET-1 results in numerous craniofacial defects. In this study we have attempted to define the point at which cephalic neural crest development is disrupted in $ET_A$-deficient embryos. We find that, while neural crest cell migration in the head of $ET_A^{-/-}$ embryos appears normal, expression of a number of transcription factors in the arch ectomesenchymal cells is either absent or significantly reduced. These $ET_A$-dependent factors include the transcription factors *goosecoid, Dlx-2, Dlx-3, dHAND, eHAND,* and *Barx1,* but not *MHox, Hoxa-2, CRABP1,* or *Ufd1.* In addition, the size of the arches in E10.5 to E11.5 $ET_A^{-/-}$ embryos is smaller and an increase in ectomesenchymal apoptosis is observed. Thus, $ET_A$ signaling in ectomesenchymal cells appears to coordinate specific aspects of arch development by inducing expression of transcription factors in the postmigratory ectomesenchyme. Absence of these signals results in retarded arch growth, defects in proper differentiation, and, in some mesenchymal cells, apoptosis. In particular, this developmental pathway appears distinct from the pathway that includes *UFD1L,* implicated as a causative gene in CATCH 22 patients, and suggests parallel complementary pathways mediating craniofacial development.   © 2000 Academic Press

*Key Words:* apoptosis; G-protein-coupled receptor; neural crest cells; pharyngeal arch.

## INTRODUCTION

The pharyngeal arches are unique transient structures that give rise to much of the head and neck skeleton (Noden, 1988). They are populated early in development by cephalic neural crest cells originating from the posterior midbrain–hindbrain region in a precise rostral–caudal pattern (Kontges and Lumsden, 1996; Lumsden *et al.*, 1991; Serbedzija *et al.*, 1992). During migration, these cells undergo an epithelial to mesenchymal transition (Le Douarin, 1982). These ectomesenchymal cells interact with epithelial and mesodermal cell populations within the arches, leading to the formation of craniofacial bones, cartilages, and connective tissues (Kontges and Lumsden, 1996; Le Douarin, 1982; Noden, 1988). Proper spatiotemporal expression of transcription factors plays a crucial role in these processes, both in guiding neural crest cells during their migration and in orchestrating their subsequent differentiation (Francis-West *et al.*, 1998).

[1] To whom correspondence should be addressed at the Howard Hughes Medical Institute, University of Texas Southwestern Medical Center, 5323 Harry Hines Blvd., Room Y5.210, Dallas, TX 75235-9050. Fax: (214) 648-5068. E-mail: afcsushi@aol.com.

We have recently demonstrated that components of the endothelin (ET) pathway are also involved in cephalic neural crest cell development. One of the two known G-protein-coupled endothelin receptors, $ET_A$, is expressed in the cephalic neural crest-derived ectomesenchyme of the pharyngeal arches (Clouthier *et al.*, 1998), while its primary ligand, endothelin-1 (ET-1), is expressed in the arch ectodermal epithelium, pharyngeal pouch endoderm, and arch core paraxial mesoderm (Clouthier *et al.*, 1998; Maemura *et al.*, 1996). Endothelin-converting enzyme-1 (ECE-1), which proteolytically converts the inactive precursor of ET-1 to the active form (Xu *et al.*, 1994), is expressed at sites both where $ET_A$ is expressed and where ET-1 is expressed (Yanagisawa *et al.*, 1998b). Targeted disruption of $ET_A$ (Clouthier *et al.*, 1998), *ET-1* (Kurihara *et al.*, 1994), or *ECE-1* (Yanagisawa *et al.*, 1998b) in mice results in craniofacial defects that resemble the human condition termed CATCH 22 (Wilson *et al.*, 1993), characterized by abnormal facies and cardiovascular defects. We have shown that the craniofacial malformations observed in $ET_A^{-/-}$ embryos is due in part to the absence of the transcription factor *goosecoid,* whose expression in the pharyngeal arches, but not in the limb buds, is disrupted in $ET_A^{-/-}$ embryos (Clouthier *et al.*, 1998). More recently, epithelial expression of both *ET-1* and *Fgf-8* were found to be crucial for proper patterning of the neural crest-derived ectomesenchyme in the caudal and rostral halves of the first arch, respectively (Tucker *et al.*, 1999). Thus, the intercellular signaling pathway mediated by ET-1/$ET_A$ interactions appears to be important for either the migration of cephalic neural crest cells or their subsequent differentiation in the arches during epithelial–mesenchymal interactions, and this effect is mediated in part through specific transcription factors.

In an attempt to further elucidate the cellular basis of craniofacial defects in $ET_A^{-/-}$ embryos, we have analyzed specific aspects of neural crest development. We find that while migration of neural crest cells into the arches of $ET_A$ mutant embryos appears unaffected, the subsequent expression of at least five transcription factors by postmigratory ectomesenchymal cells is disrupted. This indicates that disruption of $ET_A$ signaling likely affects the later events of proliferation or differentiation of neural crest derivatives, rather than crest migration. Further, expression of the factor *Dlx-3* is disrupted in both the arch mesenchyme and surrounding epithelium, suggesting a feedback loop in which epithelium-derived ET-1 induces $ET_A$ signaling within ectomesenchymal cells, which in turn results in the maintenance of *Dlx-3* expression in both the mesenchyme and the epithelium. In addition, $ET_A^{-/-}$ embryos have an increased incidence of apoptosis in the developing first arch mesenchyme, indicating that in the absence of $ET_A$-dependent developmental patterning information, at least some ectomesenchymal cells undergo programmed cell death. These findings may help in understanding the molecular and cellular basis of certain classes of human craniofacial malformations.

## MATERIALS AND METHODS

### *Mice*

Mice heterozygous for the targeted $ET_A$ allele (Clouthier *et al.*, 1998) were intercrossed in an inbred 129Sv background to produce embryos, some of which were homozygous ($ET_A^{-/-}$) for the mutation. Genotyping of embryos was also performed as previously described (Clouthier *et al.*, 1998).

### *In Situ Hybridization*

Embryos for *in situ* hybridizations were collected and fixed in 4% paraformaldehyde overnight at 4°C. Whole-mount *in situ* hybridizations were performed as previously described (Clouthier *et al.*, 1998) using digoxigenin-labeled riboprobes against *dHAND* (Srivastava *et al.*, 1997), *eHAND* (Srivastava *et al.*, 1997), *Dlx-2* (Robinson and Mahon, 1994), *Dlx-3* (Robinson and Mahon, 1994), *Barx1* (Tissier-Seta *et al.*, 1995), *MHox* (Cserjesi *et al.*, 1992; Leussink *et al.*, 1995), *Hoxa-2* (Manley and Capecchi, 1995), *CRABP-1* (Giguere *et al.*, 1990), *AP-2* (unpublished gift from T. Willimas), and *Ufd1* (Yamagishi *et al.*, 1999). Following whole-mount *in situ* hybridization, embryos were dehydrated through a graded series of ethanols, embedded in paraffin, and sectioned at 7 $\mu$m.

### *Apoptosis Analysis*

E10.5 or E11.5 wild-type, $ET_A^{+/-}$, and $ET_A^{-/-}$ embryos were collected and fixed overnight in 4% paraformaldehyde. For each age, three $ET_A^{-/-}$ and three wild-type or $ET_A^{+/-}$ embryos were examined. After processing and embedding in paraffin, 4-$\mu$m serial transverse sections through the first pharyngeal arch were cut and collected on Plus-coated slides. Following examination of unstained slides, a span of nine slides was picked for subsequent analysis. Slides 1, 4, and 7 were stained with hematoxylin and eosin (Hosoda *et al.*, 1994) and carefully examined to ensure that each pair of embryos being compared matched in both embryonic age and axial level. Embryonic age was assessed by counting the number of somites as well as by overall appearance of the embryos. The axial level chosen was through the first pharyngeal arch. While arches of $ET_A$ mutant embryos are smaller and appear developmentally delayed, the presence of specific structures was used to verify axial level. These included the second pharyngeal pouch with the entrance to the future tubotympanic recess apparent, internal carotid arteries, and inferior ganglion of the vagus (X) nerve. No gross or histological differences were observed between wild-type and $ET_A^{+/-}$ embryos. Slides 2, 5, and 8 were subjected to a TdT-mediated dUTP nick end labeling (TUNEL) assay (Gavrieli *et al.*, 1992) using the Apoptosis Detection System (Promega) and following the instructions of the manufacturer. This kit uses fluorescein-12–dUTP to label the 3′-OH ends of DNA, causing apoptotic nuclei to appear bright green when examined using fluorescence microscopy. The counterstain used was propidium iodide (Sigma) as recommended in the DNA Fragmentation Kit. This stain results in nuclei that appear red when viewed under fluorescence microscopy. Consequently, apoptotic nuclei appear yellow when a double exposure of the same section is taken. An Olympus BX-50 fluorescence microscope was used for analysis and photography.

### Quantitation of Apoptosis

To determine the apoptotic index observed in the first mandibular arch (lateral lingual swelling) of E11.5 embryos, the number of fluorescent nuclei within the first pharyngeal arch was counted, being careful to take into account fragmentation of some apoptotic nuclei. The total number of nuclei in the arch was then counted in slides 1, 4, and 7, which had been stained by hematoxylin and eosin. The apoptotic index is the total number of fluorescent nuclei as a percentage of the total number of nuclei. Statistical significance was determined using an unpaired Student's $t$ test

### Bromodeoxyuridine (BrdU) Analysis

Pregnant $ET_A^{+/-}$ female mice were injected (ip) with 200 mg of BrdU (Boehringer Mannheim) per kilogram body weight. One hour later, embryos were collected, fixed in 4% paraformaldehyde for 1 h at 4°C, and then processed for paraffin embedding. Five-micrometer paraffin sections through the first pharyngeal arch were collected on Plus-coated slides (Fisher Scientific), and every other slide was counterstained with hematoxylin and eosin to ensure that the sections examined matched those subjected to TUNEL analysis. The chosen sections were then deparaffinized and rehydrated, followed by DNA denaturation in 2 M HCl for 60 min at 37°C. The acid was neutralized by immersing slides in 0.1 M boric acid (pH 8.5), for 10 min. After being washed in PBS, sections were permeabilized in 0.3% Triton X-100 in PBS for 10 min, followed by three washes in PBS, each for 5 min. Sections were blocked in 1.5% normal horse serum (Vector) in PBS, followed by incubation with a monoclonal mouse anti-BrdU antibody (Boehringer Mannheim) at a dilution of 1:25 in 0.1% BSA in PBS overnight at 4°C. After being washed three times in PBS for 5 min each time, sections were incubated with a biotinylated horse anti-mouse antibody (Vector Laboratories) diluted to 1:2000 in 1% normal horse serum in PBS for 30 min at room temperature. The slides were washed three times in PBS for 5 min each time and then incubated with a FITC–streptavidin antibody diluted to 1:50 in PBS (pH 8.2) for 30 min in the dark. After being washed three times in PBS for 5 min each, slides were counterstained with propidium iodide (Sigma) and coverslipped using Vectabond mounting media (Vector). Under fluorescence microscopy, BrdU-positive cells have green nuclei, while all nuclei appear red from the propidium iodide. Thus, BrdU-positive nuclei appear yellow when a double exposure of the same section is taken. Negative controls included slides in which no primary or secondary antibody was used.

## RESULTS

### Normal Migration of Cephalic Neural Crest Cells in $ET_A^{-/-}$ Mice

We have previously shown that the development of cephalic neural crest derivatives is disrupted in $ET_A$ mutant embryos (Clouthier *et al.*, 1998), including the mandible, Meckel's cartilage, tympanic, gonial, jugal, alisphenoid, pterygoid, and palatine bones, as well as the malleus, incus, and hyoid. *In situ* hybridization studies showed that $ET_A$ mRNA is not observed within the neural tube, indicating that neural crest cells express $ET_A$ only after they begin migration (Clouthier *et al.*, 1998). Diffuse $ET_A$ message is then found in streams extending away from the neural tube,

presumably migrating neural crest cells, and in the head mesenchyme. Later, message is also observed in the ectomesenchyme of the pharyngeal arches. *ET-1* message is observed in the arch epithelium and core paraxial mesoderm (Clouthier *et al.*, 1998; Maemura *et al.*, 1996). The observed defects in $ET_A^{-/-}$ embryos could therefore arise as a result of aberrant migration of the crest cells or from a failure of subsequent epithelial–mesenchymal interactions of ectomesenchymal cells within the arches.

We first examined the expression of several factors known to be expressed by migrating neural crest cells. *Dlx-2,* a member of the *Distal-less* gene family, is involved in the development of proximal skeletal elements derived for arches 1 and 2 (Qiu *et al.*, 1995, 1997). Using whole-mount *in situ* hybridization analysis, *Dlx-2*-positive cells were observed extending from the posterior midbrain/anterior hindbrain into arches 1 and 2 in both E9.0 wild-type and $ET_A^{-/-}$ embryos (Fig. 1A). Similar results were obtained when we examined the expression of *AP-2,* a transcription factor crucial to the survival of migratory neural crest cells (Schorle *et al.*, 1996; Zhang *et al.*, 1996). *AP-2* expression in E9.0 wild-type and $ET_A^{-/-}$ embryos was observed in streams extending from the rhombomere (r)1/r2 region into arch 1 and r4 into arch 2 (arrows in Fig. 1B). *CRABP-1,* associated with early epithelial–mesenchymal interactions within the pharyngeal arches, was weakly expressed in the mesenchyme of arch 1 and strongly expressed in streams extending from the hindbrain into arches 2, 3, and 4 in both E9.0 wild-type and $ET_A^{-/-}$ mutant embryos (Fig. 1C). Another marker of neural crest migration into arch 2 is *Hoxa-2,* the most anteriorly expressed member of the *Hox* gene family (Gendron-Maguire *et al.*, 1993; Rijli *et al.*, 1993). *Hoxa-2* expression in migrating crest cells from r4 was also unaffected by the disruption of the $ET_A$ gene (Fig. 1D). Together, these results suggest that migration of neural crest cells from the posterior midbrain/hindbrain regions into arches 1 and 2 is not detectably affected by an absence of $ET_A$-mediated signaling. However, we cannot rule out a migratory disturbance in a small subset of neural crest cells.

### Ectomesenchymal Expression of Dlx-2 and Dlx-3 Is Abnormal in $ET_A$ Mutant Mice

Another possible effect of the absence of $ET_A$ signaling is a disruption in the molecular cues provided by transcription factors during the development of postmigratory neural crest cells within the pharyngeal arches. Thus, we examined the expression of several transcription factors in the developing arches at E9.5 and E10.5. We focused our analyses on "positional" rather than "cell type" specific markers, as we had previously shown that there were no detectable defects in the fundamental patterning of neurogenic neural crest derivatives in $ET_A^{-/-}$ embryos (Clouthier *et al.*, 1998).
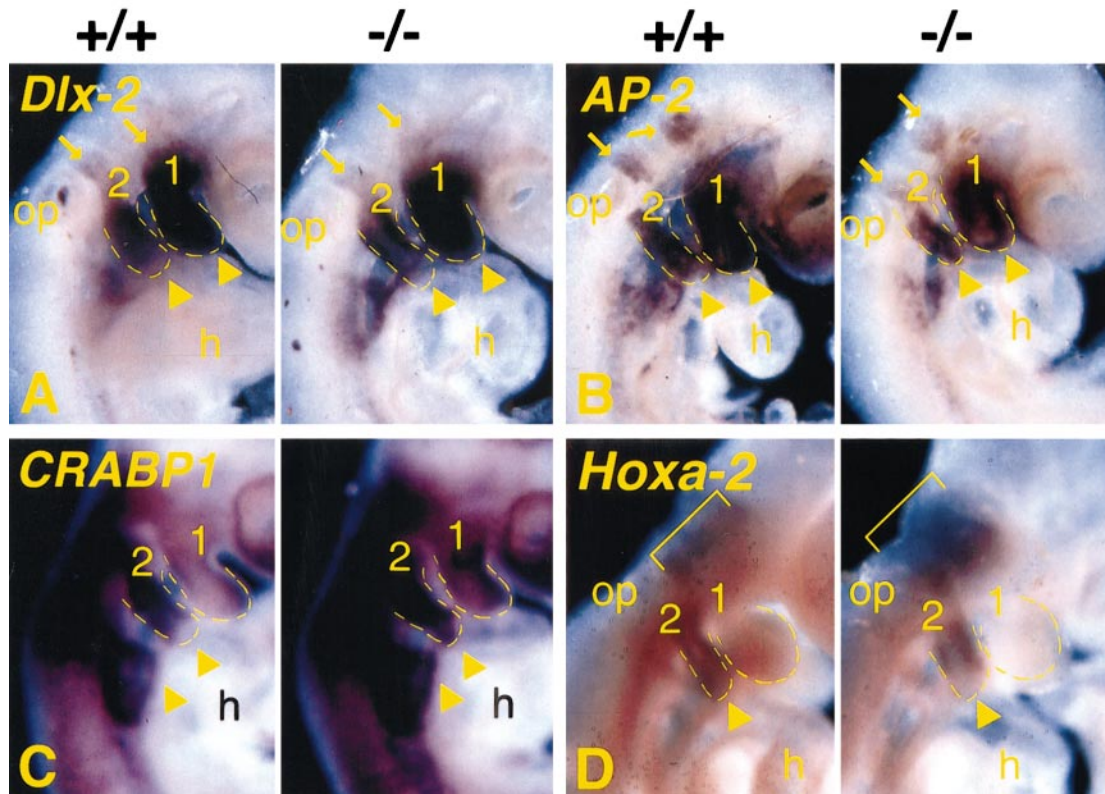
**FIG. 1.** Analysis of transcription factor expression in migrating neural crest cells in E8.75–E9.25 $ET_A^{+/+}$ and $ET_A^{-/-}$ embryos using whole-mount *in situ* hybridization. Pharyngeal arches 1 and 2 (1 and 2) are outlined in yellow to aid in visualizing their boundaries. (A) Analysis of wild-type (+/+) and mutant (−/−) embryos using a digoxigenin-labeled cRNA probe for *Dlx-2*. Yellow arrows denote expression in migrating crest cells extending from rhombomere (r) 2 and r4 into arches 1 and 2 (arrowheads) in both mutant and wild-type embryos. (B) Analysis of *AP-2* expression. Again, arrows point to migrating neural crest cells extending from r2 and r4 into arches 1 and 2 (arrowheads); no observable differences could be detected between wild-type and $ET_A^{-/-}$ embryos. (C) In both genotypes, strong *CRABP-1* expression is observed along the entire hindbrain and in arches 2 and 3 (arrowheads), with weaker expression detected in the first mandibular arch mesenchyme. (D) *Hoxa-2* expression is observed in r2–r4 (brackets) and in streams extending from r4 into arch 2 (arrowheads). Again, no differences were observed in the extent of hybridization between wild-type and $ET_A^{-/-}$ embryos. h, heart; op, otic placode.

*Dlx-2*$^{-/-}$ embryos exhibit multiple craniofacial abnormalities (Qiu *et al.*, 1995, 1997), while both *Dlx-2* and *Dlx-3* are expressed in the mesenchyme and epithelium of the arches (Robinson and Mahon, 1994; Qiu *et al.*, 1997). At E9.5, robust *Dlx-2* expression in both wild-type and $ET_A^{-/-}$ embryos was observed in the mesenchyme and epithelium of the maxillary and mandibular components of the first arch, as well as in arches 2, 3, and 4/6 (Figs. 2A and 2B). In contrast, *Dlx-3* expression, observed in epithelial (arrows in Fig. 2D) and ectomesenchymal cells in the mandibular component of arch 1 and all of arch 2 of wild-type embryos, was almost undetectable within both cell populations of E9.5 $ET_A^{-/-}$ embryos (Figs. 2C and 2D).

At E10.5, *Dlx-2* expression was observed in several locations, including arches 1, 2, and 3 in a pattern similar to that observed in E9.5 embryos (Figs. 2E and 2F). However, in E10.5 $ET_A^{-/-}$ embryos, expression of *Dlx-2* in arch 2 was absent (Figs. 2E and 2F), indicating that $ET_A$ signaling is required either for maintenance of *Dlx-2* expression in arch 2 mesenchyme or for the maintenance of the mesenchyme itself. *Dlx-3* expression in E10.5 wild-type embryos was restricted to the posterior half of arch 1 and all of arch 2, as well as in the epithelium of the nasal process (Figs. 2G and 2H). In $ET_A^{-/-}$ embryos, *Dlx-3* expression was almost completely absent in the arch mesenchyme and epithelium, although nasal epithelial expression was unchanged (arrowheads in Fig. 2H). This suggests that $ET_A$ signaling not only is necessary for mesenchymal *Dlx-3* expression but also acts in a reciprocal manner to maintain *Dlx-3* expression in the arch epithelium. It is also important to note that the sizes of arches 1 and 2 were smaller in $ET_A$ mutant embryos at E10.5, a finding observed in all subsequent whole-mount analyses and one that is indicative of a developmental defect in overall arch growth.
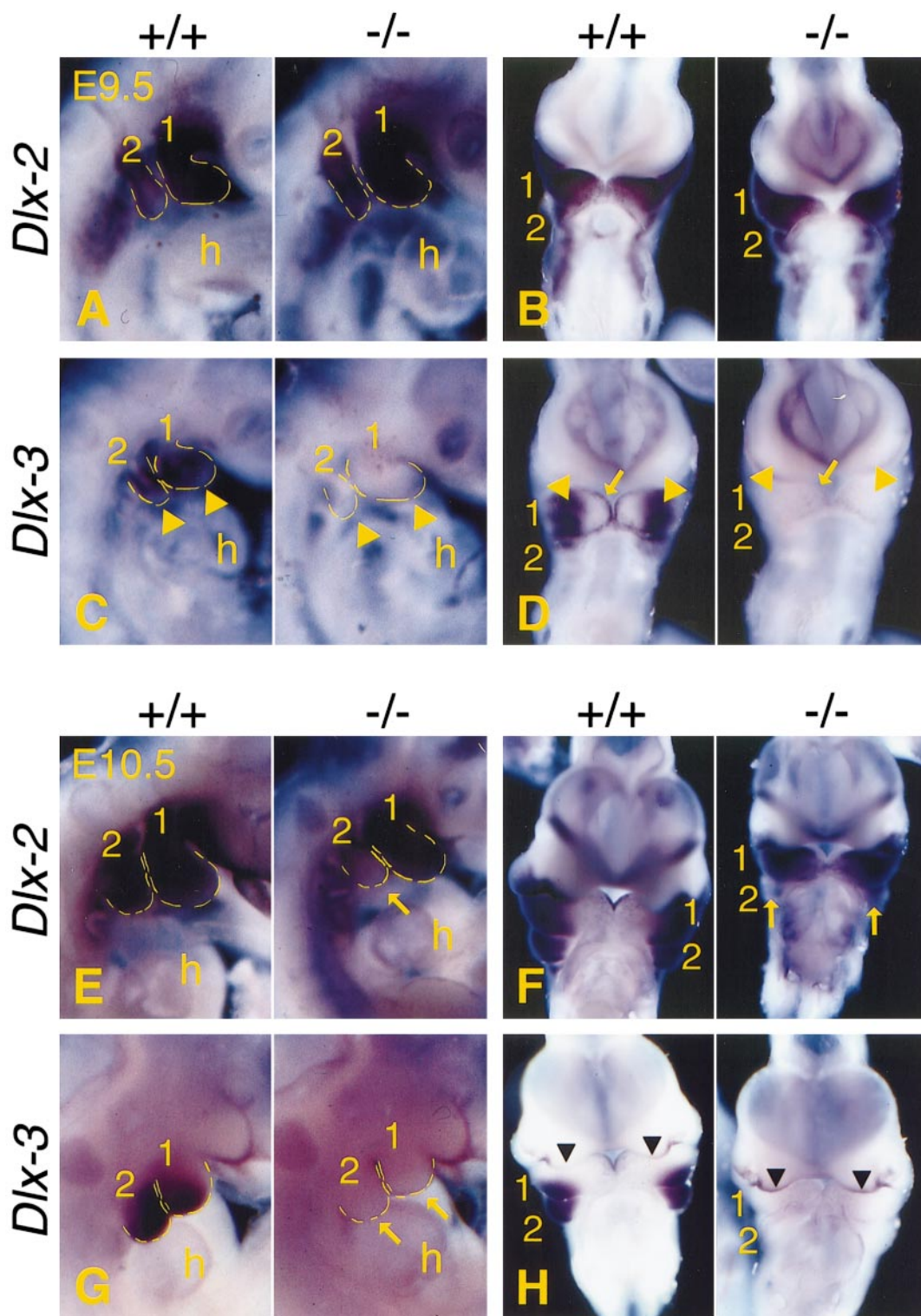
**FIG. 2.** Developmental expression patterns of two *Distal-less* genes in $ET_A{}^{-/-}$ embryos. The pharyngeal arches in A, C, E, and G are again outlined to aid with visualization. (A–H) Whole-mount *in situ* hybridization analysis using probes for *Dlx-2* and *Dlx-3* in E9.5 (A–D) and E10.5 (E–H) wild-type (+/+) and mutant (−/−) embryos. (A and B) The expression of *Dlx-2* in both the first and the second pharyngeal arches is unchanged between wild-type and mutant embryos at E9.5. (C and D) Expression of *Dlx-3* in both the mesenchyme (arrowheads in C and D) and the epithelium (arrows in D) of arches 1 and 2 is almost completely absent in E9.5 $ET_A{}^{-/-}$ embryos. (E and F). At E10.5, *Dlx-2*

## Expression of the HAND Genes Is Disrupted in $ET_A$ Mutant Mice

The transcription factors *dHAND* (Srivastava *et al.*, 1995) and *eHAND* (Cserjesi *et al.*, 1995) are expressed in both the pharyngeal arches and the conotruncal/outflow region of the heart. *dHAND* mutant embryos die around E10.5, due in part to the failure of aortic arch artery development (Srivastava *et al.*, 1997) and apoptosis of all pharyngeal arch mesenchyme (Thomas *et al.*, 1998). Further, the expression of both genes is downregulated in $ET\text{-}1^{-/-}$ embryos (Thomas *et al.*, 1998). To examine whether this was also the case in $ET_A^{-/-}$ embryos, whole-mount *in situ* hybridization analysis of *dHAND* and *eHAND* expression was examined. In E9.5 wild-type embryos, *dHAND* was expressed on the distal two-thirds of the first and second pharyngeal arches (Figs. 3A and 3B), whereas *eHAND* expression was confined to the distal one-third of the first arch (Figs. 3C and 3D). In E9.5 $ET_A^{-/-}$ embryos, the expression of both genes was nearly undetectable in the arches (Figs. 3A–3D).

At E10.5, expression of *dHAND* in wild-type embryos was observed in the mesenchyme of arches 1–6 (Figs. 3E and 3F). In $ET_A^{-/-}$ embryos, expression was almost completely absent (Figs. 3E and 3F). However, histological analysis of sectioned embryos after whole-mount *in situ* hybridization revealed that *dHAND* expression in mutant embryos was still slightly detectable within the distal aspects of the first arch mesenchyme (data not shown). Similarly, expression of *eHAND* in E10.5 wild-type embryos was unchanged from the pattern observed at E9.5, but was significantly reduced in E10.5 $ET_A^{-/-}$ embryos (Figs. 3G and 3H). However, like *dHAND* expression, *eHAND* message was still detectable along the extreme distal edge of the first arch in mutant embryos (Figs. 3G and 3H). Interestingly, expression of *dHAND* in the bilateral dorsal aortas appeared unaffected by loss of $ET_A$ signaling (yellow arrowheads in Fig. 3F), as was *dHAND* expression in the limb buds (yellow arrowheads in Fig. 3E).

## Disruption of Arch 2 Development Involves Loss of Barx1 Expression

Like *Dlx-2,* another gene showing arch 2-specific changes in expression was *Barx1,* a *BarH* family homeodomain protein initially cloned in a screen of proteins capable of binding to the *Ncam* promoter (Tissier-Seta *et al.*, 1995). In E10.5 wild-type mouse embryos, *Barx1* was expressed in the proximal aspects of the maxillary and mandibular components of the first arch and in the second arch (Figs. 4A and 4B). In E10.5 $ET_A^{-/-}$ embryos, *Barx1* expression in

the first arch was unaffected, but expression in the second arch was absent (arrows in Figs. 4A and 4B).

While we found that expression of a number of transcription factors was aberrant in $ET_A^{-/-}$ embryos, that of others was not. One gene recently implicated in the development of cephalic neural crest cells is *Ufd1*, a gene that encodes a protein involved in degradation of ubiquitinated proteins (Yamagishi *et al.*, 1999). *Ufd1* was isolated in a PCR-based subtraction screen for genes whose expression was disrupted in *dHAND* mutant embryos (Srivastava *et al.*, 1997; Thomas *et al.*, 1998). The human homolog, *UFD1L,* was mapped to 22q11 and found to be deleted in all 182 patients examined suffering from a CATCH 22 phenotype (Yamagishi *et al.*, 1999). Since *Ufd1* is presumably downstream of *dHAND,* it was assumed that its expression would be disrupted in $ET_A^{-/-}$ embryos as well. However, we found that *Ufd1* expression was unchanged in $ET_A^{-/-}$ embryos at both E9.5 (data not shown) and E10.5 (Figs. 4C and 4D), with expression observed in the frontonasal process, pharyngeal arches 1 and 2 (arrows and arrowheads in Figs. 4C and 4D), and limb buds. Though this is paradoxical, it does appear that *Ufd1* acts on a craniofacial developmental pathway separate from that of the $ET_A$ receptor.

Another molecule whose expression was unchanged was *MHox,* initially cloned in a screen of factors that bind the muscle creatine kinase enhancer (Cserjesi *et al.*, 1995). *MHox* mutant mice have defects in multiple cephalic neural crest-derived structures, indicating an involvement in the development of the ectomesenchyme (Cserjesi *et al.*, 1995). In both E10.5 wild-type and $ET_A^{-/-}$ embryos, *MHox* expression was observed throughout the first and second arches (Figs. 4E and 4F), as well as in head and limb bud mesenchyme.

## Increased Apoptosis in the First Pharyngeal Arch of $ET_A^{-/-}$ Embryos

We have previously shown that numerous arch-derived elements are either malformed or missing in E18.5 $ET_A^{-/-}$ embryos (Clouthier *et al.*, 1998). While the results described above suggest that disruption of normal transcription factor expression leads to these defects, the cellular consequences of these changes remain unknown. The size of the first arch in E11.5 wild-type embryos is clearly larger than that in $ET_A^{-/-}$ embryos (Figs. 5A and 5B). Further, the two first arch halves in E11.5 $ET_A$ mutant embryos are not yet completely fused, indicating a developmental defect. One possibility is that $ET_A$ signaling results in altered proliferation of ectomesenchymal derivatives. Alternatively, absence of $ET_A$-mediated developmental cues could lead to programmed

expression is still observed in the first arch of $ET_A^{-/-}$ embryos, but is now absent in the second arch (arrows). (G and H) Arch expression of *Dlx-3* in E10.5 $ET_A^{-/-}$ embryos is still almost completely absent (arrows in G), though expression along the nasal process epithelium at E10.5 appears similar in wild-type and mutant embryos (arrowheads in H). In frontal views (B, D, F, H), the heart has been removed in order to expose the pharyngeal arches.
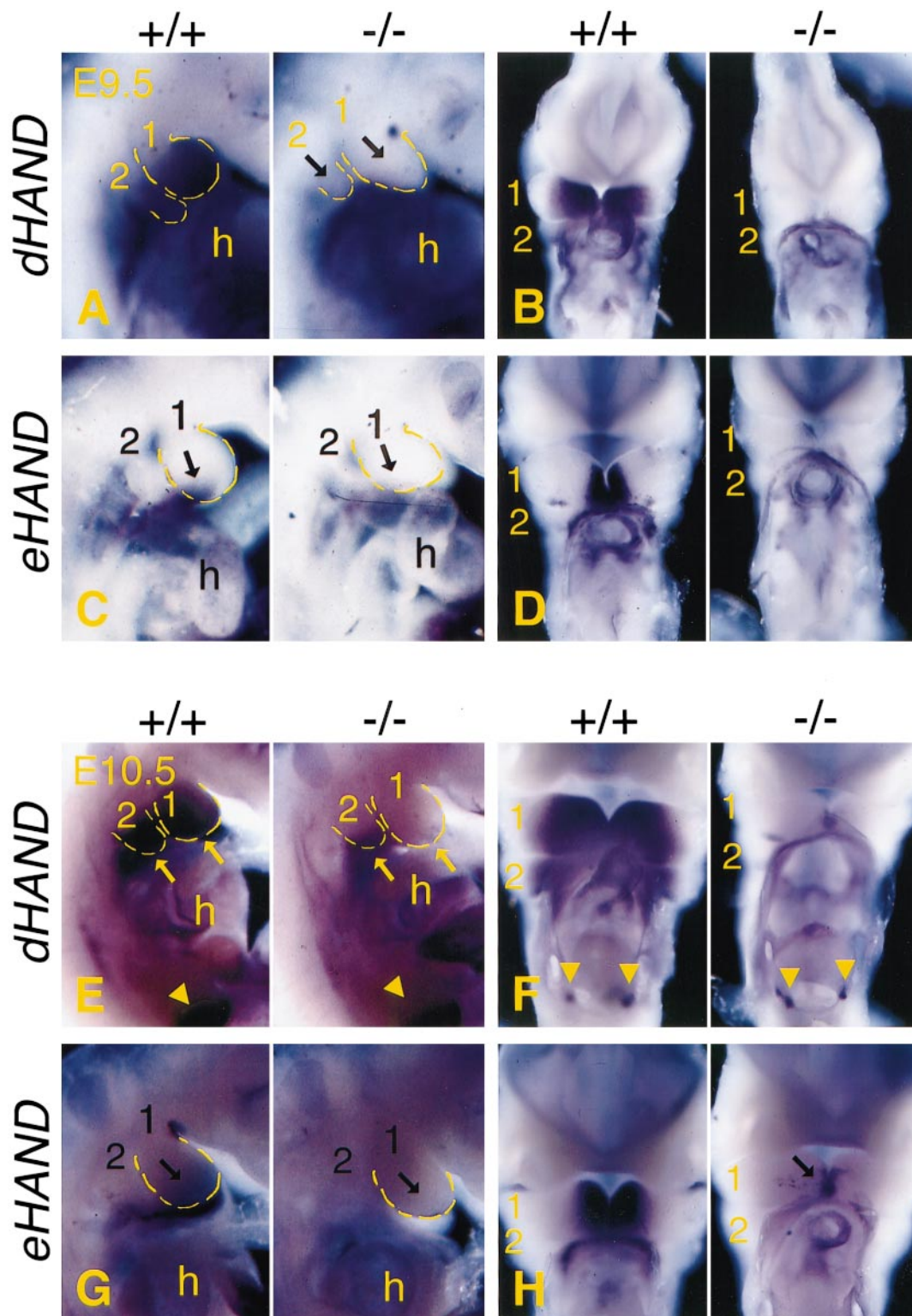
**FIG. 3.** Developmental expression patterns of the *HAND* genes in $ET_A{}^{-/-}$ embryos. (A–H) Whole-mount *in situ* hybridizations using probes for *dHAND* and *eHAND* in E9.5 (A–D) and E10.5 (E–H) wild-type (+/+) and mutant (−/−) embryos. (A and B) Expression of *dHAND* in E9.5 $ET_A{}^{-/-}$ embryos is absent in arches 1 and 2 (arrows in A). (C and D) *eHAND* expression in E9.5 $ET_A{}^{-/-}$ embryos is also significantly reduced (arrows in C). (E and F) At E10.5, *dHAND* expression is still greatly reduced in the arches of $ET_A{}^{-/-}$ embryos (arrows in E), though expression in the limb bud (arrowheads in E) and dorsal aorta (arrowheads in F) appears normal. (G and H) Arch expression of *eHAND* is still greatly reduced in $ET_A{}^{-/-}$ embryos (arrows in G and H).
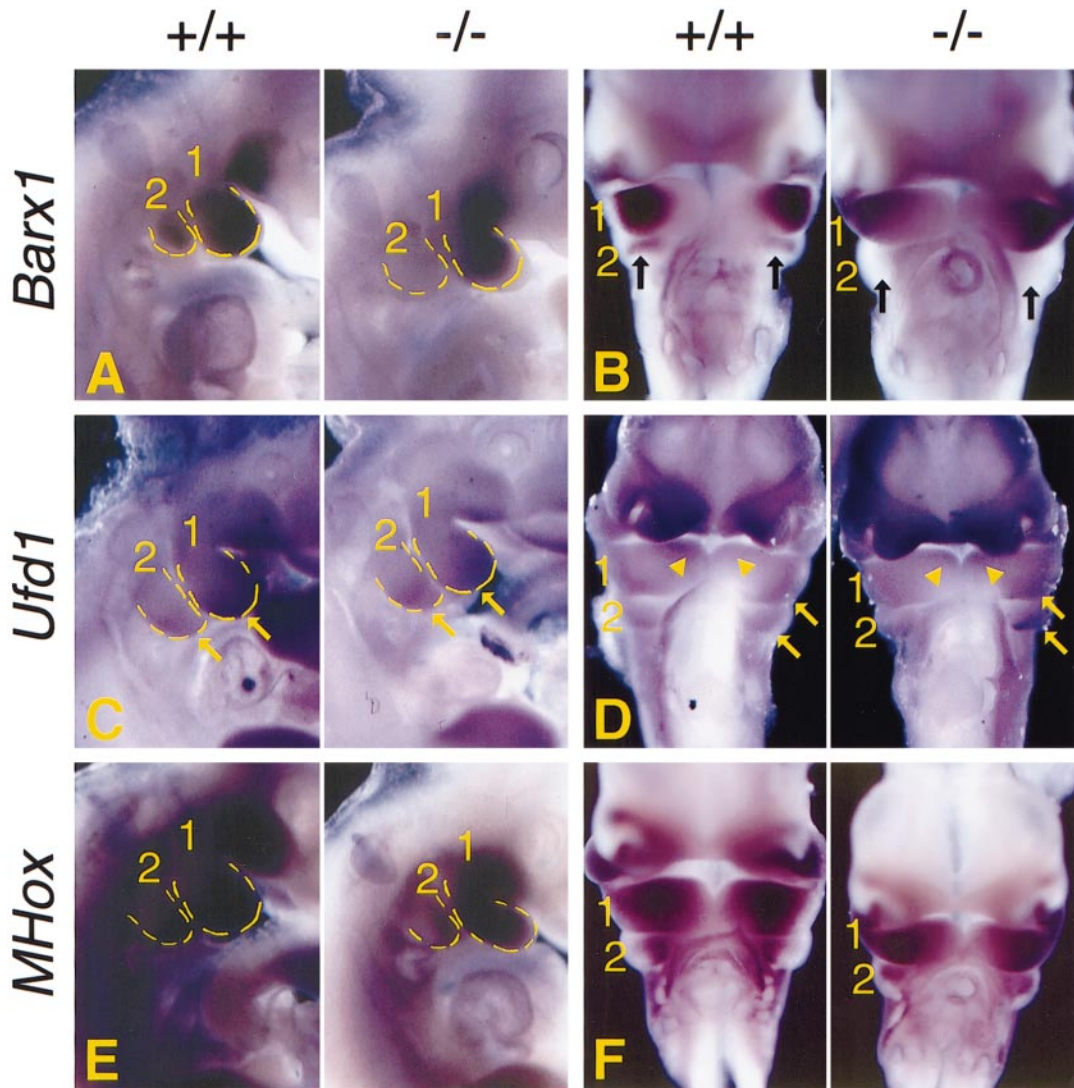
**FIG. 4.** Expression of *Barx1, Ufd1,* and *MHox* in $ET_A^{-/-}$ embryos. Whole-mount *in situ* hybridization analysis of E10.5 wild-type (+/+) and mutant (−/−) embryos. (A and B) Expression of *Barx1* is observed in the distal aspects of arches 1 and 2 in wild-type embryos, but is absent in arch 2 of $ET_A^{-/-}$ embryos (arrows in B). (C and D) In contrast, *Ufd1* expression is unchanged in $ET_A^{-/-}$ embryos, with expression observed in the pharyngeal arches (arrows in C; arrowheads and arrows in D), nasal epithelium, and limb buds. (E and F) *MHox* expression is also unchanged in $ET_A^{-/-}$ embryos; the difference in staining intensity for *MHox* is due only to slight variations in exposure time to chromogen.

cell death of a subset of ectomesenchymal cells. To explore these two possibilities, we analyzed the extent of proliferation and apoptosis within the mandibular component of the first arch at E11.5.

We first looked for changes in the gross proliferation of the mandibular arch mesenchyme at E11.5. When BrdU incorporation was examined, an obvious decrease in the number of labeled cells within the arches of $ET_A^{-/-}$ embryos was observed (Fig. 5D). This was most notable in an area extending from the proximal arch into the distal arch in $ET_A^{-/-}$ embryos (arrows in Fig. 5D). Further, arch size of mutant embryos was grossly smaller than that of wild-type

embryos, due in part to a 20% reduction in the total number of cells present (Table 1). These findings suggest that at least some ectomesenchymal cells have a reduced proliferative potential and may be the basis of the observed delayed or underdevelopment of the first arch in $ET_A$ mutant embryos.

We also examined the extent of apoptosis in the mandibular arch at E10.5 and E11.5 using the TUNEL assay (Gavrieli *et al.*, 1992). At E10.5, apoptotic nuclei were observed in the first arch of both wild-type and $ET_A^{-/-}$ embryos, most of which was associated with the normal development of the mandibular branch of the trigeminal (V)
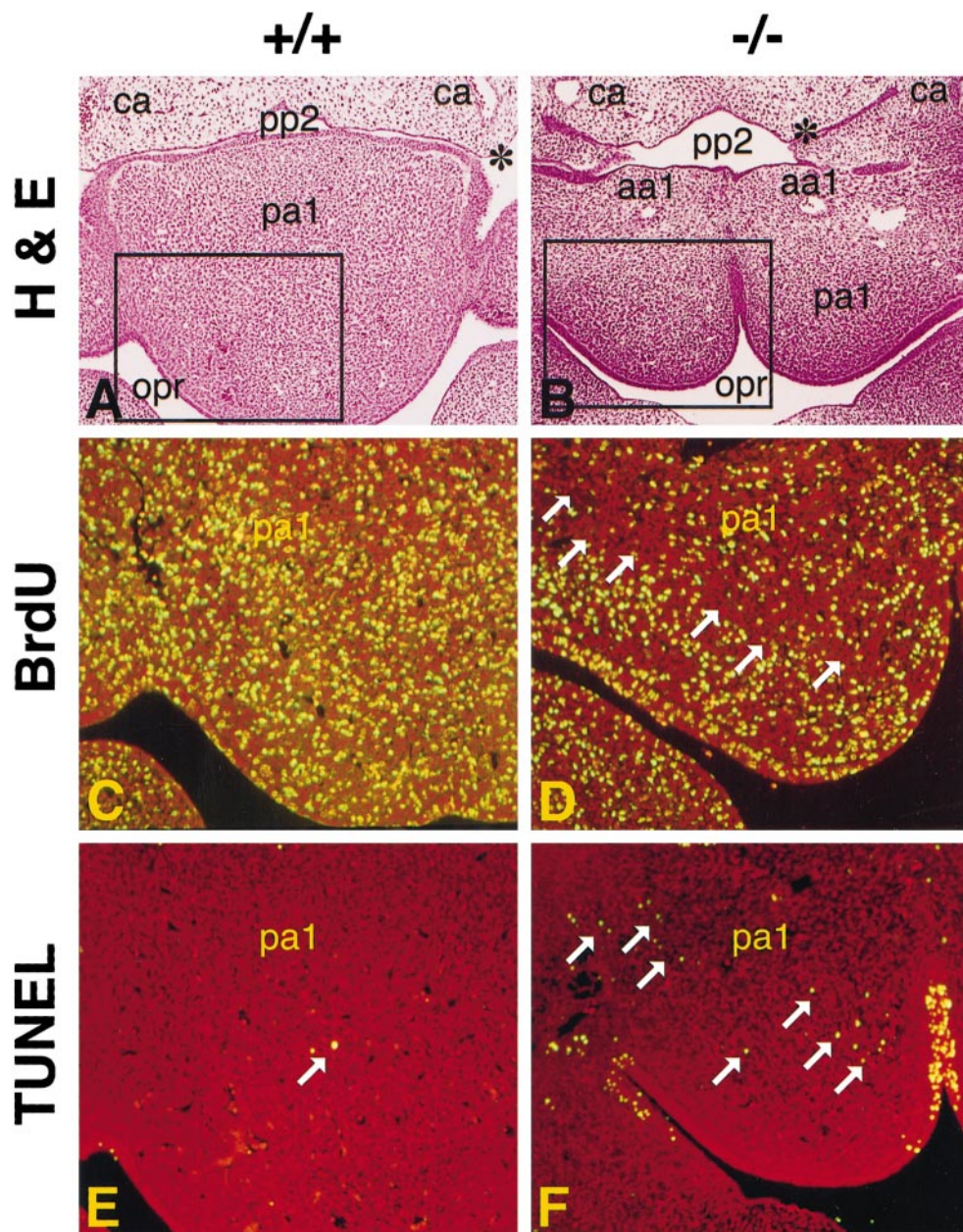
**FIG. 5.** Proliferative and apoptotic changes in E11.5 $ET_A^{-/-}$ embryos. (A–F) Sections through the transverse plane of embryos at the level of the mandibular component of the first pharyngeal arch. (A and B) Hematoxylin- and eosin-stained sections illustrate that the mandibular arch (pa1) of $ET_A^{-/-}$ embryos is significantly smaller and developmentally delayed compared with that of wild-type embryos. Landmarks used to define the axial level of the section are denoted, including the entrance of the future tubotympanic recess (asterisks) from pharyngeal pouch 2 (pp2). The areas shown in C–F are indicated with black boxes. (C and D) Bromodeoxyuridine incorporation appears less uniform in nuclei within the first arch of mutant embryos (D) than observed in wild-type embryos (C). This includes a band of nuclei in the mutant arch that extends distally across the arch (arrows). (E and F) TdT-mediated dUTP nick end labeling assay for apoptosis in $ET_A^{+/+}$ and $ET_A^{-/-}$ embryos. Yellow fluorescent nuclei indicate cells undergoing apoptosis. Significant apoptosis is observed in the arch mesenchyme of mutant embryos (arrows in F), whereas only scattered apoptotic cells are observed in the first arch of wild-type embryos (arrow in E). Due to the delayed development of the pharyngeal arches in $ET_A^{-/-}$ embryos, normal apoptosis is still observed along the fusing midline arch epithelium. These apoptotic cells were not included when calculating the apoptotic index (Table 1). aa1, aortic arch artery 1; ca, carotid artery; opr, oropharyngeal region.

**TABLE 1**

Incidence of Apoptosis in the Lateral Lingual Swelling

| Age (days) | Genotype[a] | Fluorescent nuclei | Total cells | Apoptotic index[b] |
|---|---|---|---|---|
| E11.5 | +/+ or +/− | $17.9 \pm 2.4$[c] | $4609.7 \pm 150.5$ | $0.0037 \pm 0.0004$ |
| | −/− | $55.6 \pm 3.8$* | $3775.5 \pm 122.3$** | $0.0149 \pm 0.0013$* |

[a] +/+, +/−, and −/− refer to wild-type, heterozygous, and homozygous mutant $ET_A$ embryos.
[b] The apoptotic index was obtained by dividing the number of fluorescent nuclei by the number of total cells.
[c] Numbers represent means ± standard error.
* $P < 0.0001$.
** $P = 0.0005$.

nerve (data not shown). However, by E11.5, there was a nearly fourfold increase in the incidence of apoptosis in the ectomesenchyme of $ET_A^{-/-}$ embryos (Table 1). While normal apoptosis was observed both in the pouch endoderm and along the epithelial seam between the fusing arch halves, an abnormal band of apoptotic nuclei was also found in a portion of the $ET_A^{-/-}$ arch that corresponded to the area that was BrdU deficient (Fig. 5D). Only a few apoptotic nuclei were observed in the mesenchyme of wild-type embryos (Fig. 5C). We believe that these results suggest that the absence or reduction of many of the first and second arch-derived structures in E18.5 $ET_A^{-/-}$ embryos is due in part to apoptosis of the ectomesenchymal precursors.

## DISCUSSION

Much of the head and neck skeleton arises from the cephalic neural crest-derived ectomesenchyme of the pharyngeal arches. The development of these structures is mediated in part by complex interactions of multiple transcription factors which are presumably programmed by an intricate array of intercellular signaling events. In this study, we have shown that the maintenance of expression of at least six transcription factors within the arches requires $ET_A$-mediated cell–cell signaling, a finding suggestive of a novel genetic pathway involved in craniofacial development.

### $ET_A$ Signaling Is Required by Postmigratory Neural Crest Cells

Aberrant migration of cephalic neural crest cells leads to craniofacial defects, as demonstrated in platelet-derived growth factor-$\alpha$ receptor-deficient embryos (Soriano, 1997), in which cephalic neural crest cells apparently undergo apoptosis during migration. However, our results indicate that cephalic neural crest cell migration is not significantly different between wild-type and $ET_A$ mutant embryos. These findings are also consistent with our finding that the migration of cardiac neural crest cells is also normal in $ET_A^{-/-}$ embryos (Yanagisawa *et al.*, 1998a). Rather, absence of $ET_A$ signaling appears to affect the proliferation/

differentiation of postmigratory crest cells. However, vital dye analysis of neural crest migration in $ET_A^{-/-}$ embryos will be necessary to directly prove this point.

### Hierarchical Transcription Factor Expression and Pharyngeal Arch Development

The inductive processes that modulate pharyngeal arch development are generally believed to be initiated by signals arising from the epithelium that act on ectomesenchymal cells (Hall, 1982; Tyler and Hall, 1977). Such epithelial–mesenchymal interactions within the pharyngeal arches have been documented, including CRBP-1 and CRABP-1 (Gustafson *et al.*, 1993), Msx-1 and Msx-2 (Hill *et al.*, 1989; MacKenzie *et al.*, 1991), and BMP-2 and BMP-4 (Bennett *et al.*, 1995). Our present results suggest that interaction of epithelial- and mesodermal-derived ET-1 with $ET_A$-expressing ectomesenchymal cells results in signaling that then moderates the expression of at least six transcription factors involved in head development. Figure 6 summarizes our findings by illustrating the sites at which specific transcription factors are expressed within the pharyngeal arches and where this expression is dependent on $ET_A$ signaling. From this it is clear that absent or reduced gene expression is observed primarily in more distal areas of arches 1 and 2, suggesting that $ET_A$ signaling is important for subgroups of crest cell derivatives. This might be expected, considering that *ET-1* expression is confined to the epithelium of the distal half of the pharyngeal arches as well as the paraxial mesodermal core (Clouthier *et al.*, 1998; Maemura *et al.*, 1996). However, the expression of *Dlx-2* and *Dlx-3,* both observed in more proximal arch regions, is also affected. This may reflect the presence of paracrine mediators of $ET_A$ signaling, a possibility further strengthened by the finding that maintenance of epithelial *Dlx-3* expression requires mesenchymal $ET_A$ signaling (see below). Reliance on epithelial-induced mesenchymal signals for continued epithelial development is not novel. Jernvall *et al.* demonstrated that during tooth development epithelial-derived BMP-4 expression is required for maintenance of epithelial function, but is transduced through mesenchymal signals (Msx-1 and Msx-2) (Jernvall *et al.*, 1998). Whether the expression of other epithelial factors is

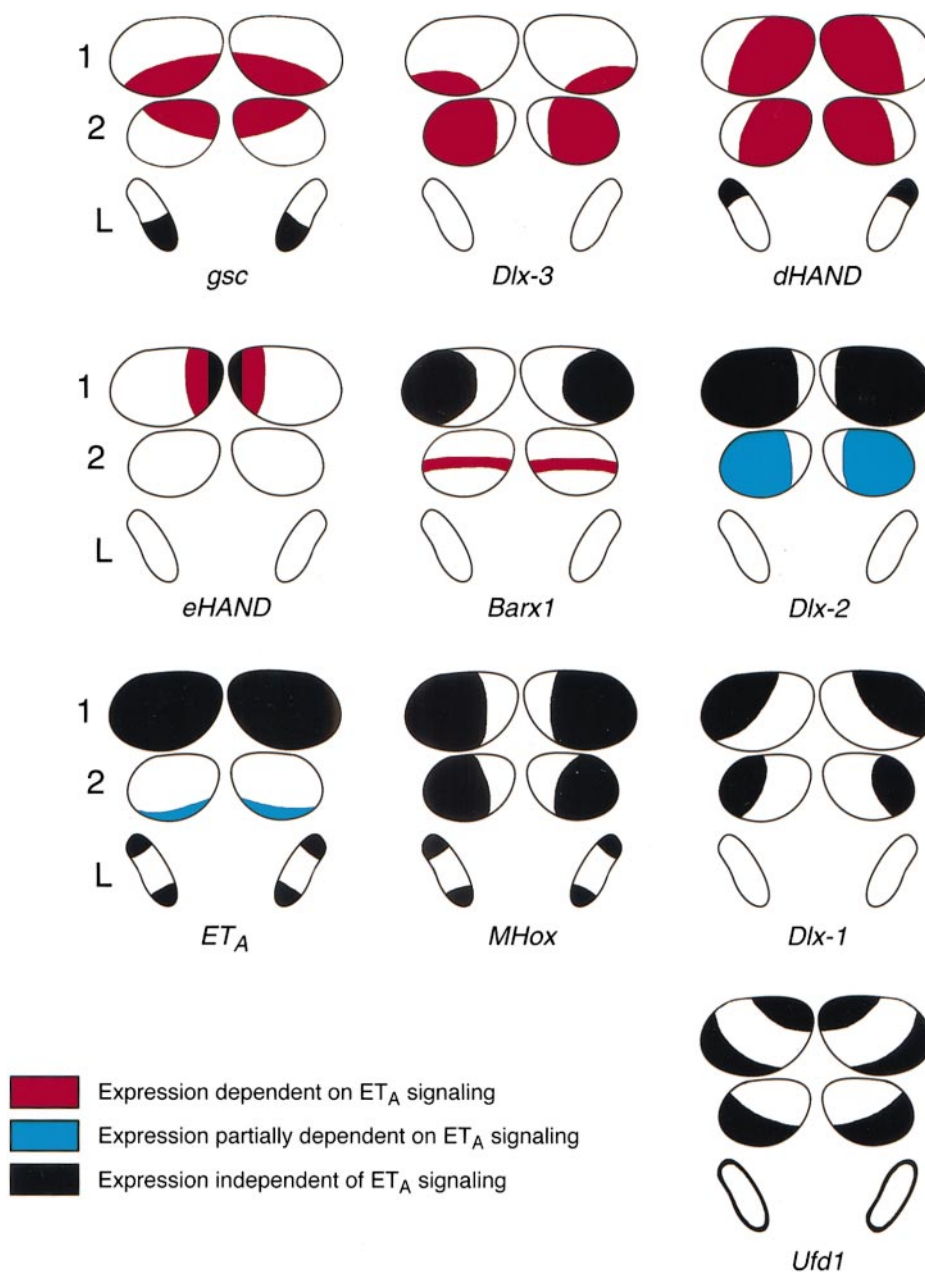**FIG. 6.** Expression domains of various transcription factors involved in craniofacial development. Areas depicted in red depend on $ET_A$ signaling for initiation or maintenance of expression, whereas areas shown in blue are dependent on $ET_A$ signaling for maintenance of expression. Black areas depict domains where transcription factor expression is independent of $ET_A$ signaling. L, limb bud.

affected in $ET_A$-deficient mice or what the nature of a paracrine mediator might be is not yet known.

It is currently not clear how many signaling pathways govern craniofacial development. Since *Dlx-1, Hoxa-2,* and *MHox* are all properly expressed in $ET_A^{-/-}$ embryos, these factors could either act upstream of $ET_A$ signaling or belong to different or parallel genetic pathways governing pharyn-

geal arch development. The spatiotemporal expression patterns of these molecules argues for the latter explanation. These additional pathways most likely work in concert with the $ET_A$ pathway in patterning the head, as mice mutant for *Dlx-1* (Qiu *et al.*, 1997), *Hoxa-2* (Gendron-Maguire *et al.*, 1993; Rijli *et al.*, 1993), or *MHox* (Martin *et al.*, 1995) all share at least a subset of missing or deformed

elements with $ET_A^{-/-}$ embryos. It will be important to examine the expression of other transcription factors as well as $ET_A$ expression in *Dlx-1, Hoxa-2,* and *MHox* mutant mice to address these questions further.

## Proliferative and Apoptotic Changes in $ET_A^{-/-}$ Embryos

One of the first observable morphological defects in $ET_A^{-/-}$ embryos is reduced mandibular and hyoid arch size, noticeable at E10.5. Our BrdU and TUNEL staining results suggest that this may be partly due to slowed proliferation of arch mesenchymal cells and their subsequent removal through apoptosis. Increased ectomesenchymal apoptosis likely reflects a loss of normal environmental cues in ectomesenchymal cells, rather than suggesting that $ET_A$ signaling normally has a direct antiapoptotic effect. This is based on the fact that significantly elevated apoptosis is not observed until E11.5 in $ET_A^{-/-}$ embryos, even though $ET_A$ is normally expressed as early as E8.5 (our unpublished data). Yet, questions remain concerning how these changes are brought about. One hypothesis is that the absence of environmental cues (transcription factors) results in a stress response which then results in both slowed progression through S phase and later, apoptosis. p21, which inhibits cell proliferation at the $G_1/S$ transition point (Harper and Elledge, 1996), has been shown to be involved in early tooth remodeling during epithelial–mesenchymal interactions (Jernvall *et al.*, 1998) and in mediating stress-induced proliferative and apoptotic changes *in vitro* (Gorospe *et al.*, 1996), so it is an attractive molecule to consider. It is also possible that the aberrant expression of cell cycle factors themselves leads to reduced proliferation and apoptosis. Analysis of molecules associated with cell cycle control and apoptosis will have to be examined in $ET_A^{-/-}$ ectomesenchymal cells to determine if these possibilities are occurring.

It is somewhat surprising that ectomesenchymal apoptosis is not more striking, considering the complex and multifaceted craniofacial phenotype observed in $ET_A^{-/-}$ embryos (Clouthier *et al.*, 1998). Further, absence of *dHAND* expression in *dHAND*$^{-/-}$ embryos resulted in disruption of *Msx-1* expression and massive apoptosis of arch mesenchymal cells by E10.5 (Thomas *et al.*, 1998). Why then is arch apoptosis not more widespread in $ET_A^{-/-}$ embryos? Thomas *et al.* show that *Msx-1* expression is normal in *ET-1*$^{-/-}$ embryos and thus speculate that the apoptosis in *dHAND* mutant embryos results from absence of *Msx-1* expression. In their model, residual *dHAND* expression observed in *ET-1*-deficient embryos, similar to the expression level observed in $ET_A^{-/-}$ embryos, is sufficient to induce or maintain *Msx-1* expression in *ET-1*$^{-/-}$ embryos and thus protect against ectomesenchymal apoptosis. However, functional inactivation of *Msx-1* in mice does not result in widespread loss of arch-derived elements (Satokata and Maas, 1994), implying that loss of *Msx-1* alone does not result in ectomesenchymal apoptosis. Also,

the proposed action of *Msx-1* during epithelial–mesenchymal interactions that occur during tooth development suggests that absence of *Msx-1* might actually have an antiapoptotic affect (Jernvall *et al.*, 1998). Thus, this evidence indicates that loss of *Msx-1* expression alone does not directly correlate with ectomesenchymal apoptosis, though the mechanism for its differential regulation in *ET-1*$^{-/-}$ (and presumably $ET_A^{-/-}$) and *dHAND*$^{-/-}$ embryos is not clear (see below).

Scattered apoptosis in the mesenchyme of $ET_A$ mutant embryos may reflect a differential dependence on $ET_A$ signaling by subgroups of neural crest cells, possibly representing their rhombomeric origin (Kontges and Lumsden, 1996), and could explain the absence of *Barx1, Dlx-2,* and truncated $ET_A$ transcripts only in the second arch. This may also explain the fact that not all arch-derived elements are missing in term embryos; many structures are simply malformed. This may result from the action of other signaling pathways that can partially compensate for the loss of $ET_A$ signaling, preventing widespread apoptosis of ectomesenchymal cells but not entirely rescuing their abnormal development. Analysis of the developmental potential of $ET_A^{-/-}$ cells in $ET_A^{+/+} \leftrightarrow ET_A^{-/-}$ chimeric embryos may help clarify these points.

## Possible Functions of Dlx-2, Dlx-3, and dHAND Downstream of $ET_A$ Signaling

The differential change in *Dlx-2* expression between the first and the second arches of $ET_A^{-/-}$ embryos is intriguing and may provide insight into the role of *Dlx-2* downstream of $ET_A$ signaling. *Dlx-2*$^{-/-}$ mice exhibit abnormal development of cranial bones derived from the proximal aspects of arches 1 and 2, including the alisphenoid and maxillary bones (arch 1) and the stapes and styloid (arch 2) (Qui *et al.*, 1995). *Dlx-2* is thus believed to be crucial for proper proximodistal patterning of the arches. While absence of $ET_A$ signaling affects most arch-derived elements (Clouthier *et al.*, 1998), distal structures of the first arch are more severely affected, with most being completely absent (i.e., Meckel's cartilage, the mandible, and the malleus). This correlates with higher epithelial *ET-1* expression in the medial–distal aspects of the arch (Maemura *et al.*, 1996). This does not, however, explain the loss of *Dlx-2* expression in the second arch, which suggests that $ET_A$ signaling is either directly or indirectly inducing a second arch-specific mediator of *Dlx-2* expression. It is interesting that the major phenotypic overlap between *Dlx-2*$^{-/-}$ and $ET_A^{-/-}$ embryos is severe malformation or absence of the stapes and styloid. Thus, this may represent a signaling axis involved in patterning of these two craniofacial structures.

The effects of Dlx-3 absence in $ET_A^{-/-}$ embryos are more difficult to assess due to the early embryonic lethality of *Dlx-3*$^{-/-}$ embryos (Morasso *et al.*, 1999). Like *Dlx-2, Dlx-3* is expressed in the proximal aspects of arches 1 and 2, with first-arch expression becoming restricted to the caudal half by E10.0 (Robinson and Mahon, 1994). This caudal restric-

tion resembles a pattern observed for a subpopulation of cephalic crest cells derived from rhombomeres 1 and 2 (Lumsden *et al.*, 1991). Long-term fate mapping analysis indicates that this subpopulation eventually forms the incus (Kontges and Lumsden, 1996). Thus, *Dlx-3* may be involved in incus development, and downregulation of *Dlx-3* expression as a direct or indirect consequence of loss of $ET_A$ receptor signaling in $ET_A^{-/-}$ embryos may therefore contribute to the absence of the incus. The expression pattern of *Dlx-3* in the second arch indicates that it may be involved with *Dlx-2* in the development of the stapes and styloid.

Another interesting aspect of *Dlx-3* expression is that it is not only absent in the mesenchyme, but is also greatly reduced in the arch epithelium of $ET_A^{-/-}$ embryos. During arch development, proliferation of the ectodermal epithelium occurs concomitantly with ectomesenchymal proliferation, ensuring proportional growth. Growth and maintenance of the epithelium also have a more direct impact on head development, as the ectoderm is believed to be involved in the development of the cephalic neural crest-derived dermal bones, including the jugal and squamosal bones (Tyler and Hall, 1977), two bones that are malformed in $ET_A^{-/-}$ embryos (Clouthier *et al.*, 1998). Epithelial expression of *Dlx-3* has been hypothesized to be involved in dermal bone development (Qiu *et al.*, 1997), and its absence may thus be a major contributing factor to dermal bone deformities observed in $ET_A^{-/-}$ embryos. Interestingly, a mutation in *DLX-3* has recently been found to be associated with trichodento-osseous syndrome in humans, an autosomal dominant disorder primarily affecting the teeth and cranial bones (Price *et al.*, 1998). The sites of this disease occur in areas in which significant epithelial–mesenchymal interactions occur during development, illustrating the importance of *Dlx-3* in epithelial–mesenchymal interactions during head development.

Another interesting relationship is that of $ET_A$ and dHAND. Although normal *dHAND* expression is dependent on $ET_A$ signaling, and expression of both *Ufd1* and *Msx-1* is dependent on *dHAND,* we and others (H. Kurihara, personal communication) have found that *Ufd1* expression is intact in *ET-1*$^{-/-}$ and $ET_A^{-/-}$ embryos, as is *Msx-1* expression in *ET-1*$^{-/-}$ embryos (and thus presumably in $ET_A^{-/-}$ embryos) (Thomas *et al.*, 1998). This is despite the fact that *UFD1L* mutations in humans (CATCH 22) result in a phenotype that closely resembles that of $ET_A^{-/-}$ embryos (Clouthier *et al.*, 1998; Yamagishi *et al.*, 1999). We currently do not understand the basis of these discrepancies, though the cardiac insufficiency observed in *dHAND* mutant embryos that leads to death at E11.0 may contribute to changes throughout the embryo, including the heart and pharyngeal arches. These changes would likely include the loss of expression of numerous genes, many of which would not necessarily lie directly downstream of *dHAND.* In contrast, while loss of $ET_A$ signaling disrupts cephalic and cardiac neural crest cell development, embryonic lethality is not observed. Therefore, widespread changes in gene

expression would not be expected. That *Ufd1* expression is normal in $ET_A^{-/-}$ embryos also illustrates the complex combinatorial pathways that are required for correct craniofacial patterning and suggests that other 22q11 genes may act downstream of $ET_A$ signaling. Further analysis of *Msx-1* and *Ufd1,* as well as other downstream signaling molecules of $ET_A$ and *dHAND,* will be necessary to better understand these processes.

## REFERENCES

Bennett, J. H., Hunt, P., and Thorogood, P. (1995). Bone morphogenetic protein-2 and -4 expression during murine orofacial development. *Arch. Oral Biol.* **40,** 847–854.

Clouthier, D. E., Hosoda, K., Richardson, J. A., Williams, S. C., Yanagisawa, H., Kuwaki, T., Kumada, M., Hammer, R. E., and Yanagisawa, M. (1998). Cranial and cardiac neural crest defects in endothelin-A receptor-deficient mice. *Development* **125,** 813–824.

Cserjesi, P., Brown, D., Lyons, G. E., and Olson, E. N. (1995). Expression of the novel basic helix-loop-helix gene *eHAND* in neural crest derivatives and extraembryonic membranes during mouse development. *Dev. Biol.* **170,** 664–678.

Cserjesi, P., Lilly, B., Bryson, L., Wang, Y., Sassoon, D. A., and Olson, E. N. (1992). MHox: A mesodermally restricted homeodomain protein that binds an essential site in the muscle creatine kinase enhancer. *Development* **115,** 1087–1101.

Francis-West, P., Ladher, R., Barlow, A., and Graveson, A. (1998). Signalling interactions during facial development. *Mech. Dev.* **75,** 3–28.

Gavrieli, Y., Sherman, Y., and Ben-Sasson, S. A. (1992). Identification of programmed cell death in situ via specific labeling of nuclear DNA fragmentation. *J. Cell Biol.* **119,** 493–501.

Gendron-Maguire, M., Mallo, M., Zhang, M., and Gridley, T. (1993). *Hoxa-2* mutant mice exhibit homeotic transformation of skeletal elements derived from cranial neural crest. *Cell* **75,** 1317–1331.

Giguere, V., Lyn, S., Yip, P., Siu, C. H., and Amin, S. (1990). Molecular cloning of cDNA encoding a second cellular retinoic acid-binding protein. *Proc. Natl. Acad. Sci. USA* **87,** 6233–6237.

Gorospe, M., J. L., M., M. S., S., Fornace, A. L. J., and Holbrook, N. J. (1996). Regulation of p21 super(CIP1/WAF1) expression by cellular stress: p53-dependent and p53-independent mechanisms. *Mol. Cell. Differ.* **4,** 47–65.

Gustafson, A.-L., Dencker, L., and Eriksson, U. (1993). Nonoverlapping expression of CRBP 1 and Crabp 1 during pattern

formation of limbs and craniofacial structures in the early mouse embryo. *Development* **117,** 451–460.

Hall, B. K. (1982). Mandibular morphogenesis and craniofacial malformations. *J. Craniofac. Genet. Dev. Biol.* **2,** 309–322.

Harper, J. W., and Elledge, S. J. (1996). cdk inhibitors in development and cancer. *Curr. Opin. Genet. Dev.* **6,** 56–64.

Hill, R. E., Jones, R. F., Rees, A. R., Sime, C. M., Copeland, N. G., Jenkins, N. A., Graham, E., and Davidson, D. R. (1989). A new family of mouse homeobox containing genes: Molecular structure, chromosomal location and developmental expression of *Hox-7.1. Genes Dev.* **3,** 26–37.

Hosoda, K., Hammer, R. E., Richardson, J. A., Baynash, A. G., Cheung, J. C., Giaid, A., and Yanagisawa, M. (1994). Targeted and natural (piebald-lethal) mutations of endothelin-B receptor gene produce megacolon associated with spotted coat color in mice. *Cell* **79,** 1267–1276.

Jernvall, J., Aberg, T., Kettunen, P., Deranen, S., and Thesleff, I. (1998). The life history of an embryonic signaling center: BMP-4 induces *p21* and is associated with apoptosis in the mouse tooth enamel knot. *Development* **125,** 161–169.

Kontges, G., and Lumsden, A. (1996). Rhombencephalic neural crest segmentation is preserved throughout craniofacial ontogeny. *Development* **122,** 3229–3242.

Kurihara, Y., Kurihara, H., Suzuki, H., Kodama, T., Maemura, K., Nagai, R., Oda, H., Kuwaki, T., Cao, W.-H., Kamada, N., Jishage, K., Ouchi, Y., Azuma, S., Toyoda, Y., Ishikawa, T., Kumada, M., and Yazaki, Y. (1994). Elevated blood pressure and craniofacial abnormalities in mice deficient in endothelin-1. *Nature* **368,** 703–710.

Le Douarin, N. M. (1982). "The Neural Crest." Cambridge Univ. Press, Cambridge, UK.

Leussink, B., Brouwer, A., El Khattabi, M., Poelmann, R. E., Gittenberger-deGroot, A. C., and Meijlink, F. (1995). Expression patterns of the paired-related homeobox genes *MHox/Prx1* and *S8/Prx2* suggest roles in development of the heart and the forebrain. *Mech. Dev.* **52,** 51–64.

Lumsden, A., Sprawson, N., and Graham, A. (1991). Segmental origin and migration of neural crest cells in the hindbrain region of the chick embryo. *Development* **113,** 1281–1291.

MacKenzie, A., Ferguson, M. W. J., and Sharpe, P. T. (1991). Hox-7 expression during murine craniofacial development. *Development* **113,** 601–611.

Maemura, K., Kurihara, H., Kurihara, Y., Oda, H., Ishikawa, T., Copeland, N. G., Gilbert, D. J., Jenkins, N. A., and Yazaki, Y. (1996). Sequence analysis, chromosomal location, and developmental expression of the mouse preproendothelin-1 gene. *Genomics* **31,** 177–184.

Manley, N. R., and Capecchi, M. R. (1995). The role of *Hoxa-3* in mouse thymus and thyroid development. *Development* **121,** 1989–2003.

Martin, J. F., Bradley, A., and Olson, E. N. (1995). The *paired*-like homeo box gene *MHox* is required for early events of skeletogenesis in multiple lineages. *Genes Dev.* **9,** 1237–1249.

Morasso, M. I., Grinberg, A., Robinson, G., Sargent, T. D., and Mahon, K. A. (1999). Placental failure in mice lacking the homeobox gene Dlx3. *Proc. Natl. Acad. Sci. USA* **96,** 162–167.

Noden, D. M. (1988). Interactions and fates of avian craniofacial mesenchyme. *Development* **103,** 121–140.

Price, J. A., Bowden, D. W., Wright, J. T., Pettenati, M. J., and Hart, T. C. (1998). Identification of a mutation in *DLX3* associated with tricho-dento-osseous (TDO) syndrome. *Hum. Mol. Genet.* **7,** 563–569.

Qiu, M., Bulfone, A., Ghattas, I., Meneses, J. J., Christensen, L., Sharpe, P. T., Presley, R., Pedersen, R. A., and Rubenstein, J. L. R. (1997). Role of the Dlx homeobox genes in proximodistal patterning of the branchial arches: Mutations of Dlx-1, Dlx-2, and Dlx-1 and -2 alter morphogenesis of proximal skeletal and soft tissue structures derived from the first and second arches. *Dev. Biol.* **185,** 165–184.

Qui, M., Bulfone, A., Martinez, S., Meneses, J. J., Shimamura, K., Pedersen, R. A., and Rubenstein, J. L. R. (1995). Null mutation of *Dlx-2* results in abnormal morphogenesis of proximal first and second branchial arch derivatives and abnormal differentiation in the forebrain. *Genes Dev.* **9,** 2523–2538.

Rijli, F. M., Mark, M., Lakkaraju, S., Dierich, A., Dolle, P., and Chambon, P. (1993). A homeotic transformation is generated in the rostral branchial region of the head by disruption of *Hoxa-2,* which acts as a selector gene. *Cell* **75,** 1333–1349.

Robinson, G. W., and Mahon, K. A. (1994). Differential and overlapping expression domains of *Dlx-2* and *Dlx-3* suggest distinct roles for *Distal-less* homeobox genes in craniofacial development. *Mech. Dev.* **48,** 199–215.

Satokata, I., and Maas, R. (1994). *Msx1* deficient mice exhibit cleft palate and abnormalities of craniofacial and tooth development. *Nat. Genet.* **6,** 348–356.

Schorle, H., Meier, P., Buchert, M., Jaenisch, R., and Mitchell, P. J. (1996). Transcription factor AP-2 essential for cranial closure and craniofacial development. *Nature* **381,** 235–238.

Serbedzija, G. N., Bronner-Fraser, M., and Fraser, S. E. (1992). Vital dye analysis of cranial neural crest cell migration in the mouse embryo. *Development* **116,** 297–307.

Soriano, P. (1997). The PDGFα receptor is required for neural crest cell development and for normal patterning of the somites. *Development* **124,** 2691–2700.

Srivastava, D., Cserjesi, P., and Olson, E. N. (1995). A subclass of bHLH proteins required for cardiac morphogenesis. *Science* **270,** 1995–1999.

Srivastava, D., Thomas, T., Lin, Q., Kirby, M. L., Brown, D., and Olson, E. N. (1997). Regulation of cardiac mesodermal and neural crest development by the bHLH transcription factor, dHAND. *Nat. Genet.* **16,** 154–160.

Thomas, T., Kurihara, H., Yamagishi, H., Kurihara, Y., Yazaki, Y., Olson, E. N., and Srivastava, D. (1998). A signaling cascade involving endothelin-1, dHAND and Msx1 regulates development of neural-crest-derived branchial arch mesenchyme. *Development* **125,** 3005–3014.

Tissier-Seta, J.-P., Mucchielli, M.-L., Mark, M. M.-G., Goridis, C., and Brunet, J.-F. (1995). *Barx1,* a new mouse homeodomain transcription factor expressed in cranio-facial ectomesenchyme and the stomach. *Mech. Dev.* **51,** 3–15.

Tucker, S. A., Yamada, G., Grigoriou, M., Pachnis, V., and Sharpe, P. T. (1999). Fgf-8 determines rostral–caudal polarity in the first branchial arch. *Development* **126,** 51–61.

Tyler, M. S., and Hall, B. K. (1977). Epithelial influences on skeletogenesis in the mandible of the embryonic chick. *Anat. Rec.* **188,** 229–240.

Wilson, D. I., Burn, J., Scambler, P., and Goodship, J. (1993). DiGeorge syndrome: Part of CATCH 22. *J. Med. Genet.* **30,** 852–856.

Xu, D., Emoto, N., Giaid, A., Slaughter, C., Kaw, S., deWit, D., and Yanagisawa, M. (1994). ECE-1: A membrane-bound metalloprotease that catalyzes the proteolytic activation of big endothelin-1. *Cell* **78,** 473–85.

Yamagishi, H., Garg, V., Matsuoka, R., Thomas, T., and Srivastava, D. (1999). A molecular pathway revealing a genetic basis for human cardiac and craniofacial defects. *Science* **283,** 1158–1161.

Yanagisawa, H., Hammer, R. E., Richardson, J. A., Williams, S. C., Clouthier, D. E., and Yanagisawa, M. (1998a). Role of endothelin-1/endothelin-A receptor-mediated signaling pathway in the aortic arch patterning in mice. *J. Clin. Invest.* **102,** 22–33.

Yanagisawa, H., Yanagisawa, M., Kapur, R. P., Richardson, J. A., Williams, S. C., Clouthier, D. E., de Wit, D., Emoto, N., and Hammer, R. E. (1998b). Dual genetic pathways of endothelin-mediated intercellular signaling revealed by targeted disruption

of endothelin converting enzyme-1 gene. *Development* **125,** 825–836.

Zhang, J., Hagopian-Donaldson, S., Serbedzija, G., Elsemore, J., Plehn-Dujowich, D., McMahon, A. P., Flavell, R. A., and Williams, T. (1996). Neural tube, skeletal and body wall defects in mice lacking transcription factor AP-2. *Nature* **381,** 238–241.